Electroluminescence Color Tuning by Dye Doping in Organic Light-Emitting Diodes

Andrei A. Shoustikov, Yujian You, and Mark E. Thompson

(Invited Paper)

Abstract—Doping a small amount of a fluorescent dye into an organic light-emitting diodes (OLED's) can lead to significant changes in the color of luminescence and an improvement in the device properties (e.g., quantum efficiency, lifetime, etc.). The process of energy transfer from the OLED material to the dye in these devices may involve several different processes, including carrier trapping as well as Förster and Dexter energy transfer reactions. The important parameters for each of these processes are discussed. The color purity and chromaticities of a wide range of different dye-doped OLED's are reviewed.

Index Terms—Chromaticity, color tuning, Dexter, doping, emission energy, energy transfer, Förster, luminescent dye.

I. INTRODUCTION

CONSIDERABLE research is currently focused on the development of new light-emitting device technologies for flat panel displays. The primary motivation is to replace bulky and energy consuming cathode ray tubes (CRT's) with energy efficient flat panels. Liquid crystal displays (LCD's) are a reasonable substitute for CRT's in some applications, however, it would be advantageous for ease of viewing in bright background environments to have an emissive display, rather than the reflective or transmissive panels of LCD's. One emissive technology that shows promise involves organic light-emitting diodes (OLED's). There are early reports of OLED's built from molecular crystals [1]–[4], but the first efficient OLED utilized vapor deposited thin films, emitting green electroluminescence (EL) from aluminum tris(8-hydroxyquinoline) (Alq$_3$) [5], [6]. A wide range of materials have been subsequently reported that efficiently produce EL throughout the visible spectrum. While the color of light emission can readily be controlled by altering the materials that make up the device, this can often lead to decreased efficiencies and broad lines. An alternate method of color tuning in OLED's involves doping small amounts of photoluminescent (PL) dyes into the OLED structure. The dye in this device intercepts the excitons formed in the OLED and emits on its own. The first report of electroluminescence from a dye dopant in a molecular organic matrix concerned a tetracene dopant in anthracene [1]. This device gave exclusively tetracene emission, but at a drive voltage of more than 400 V. OLED's have improved significantly since that report and the use of

dye dopants has improved with them [7]–[10]. The PL dye doping technique has been used to fabricate OLED's whose colors span the entire visible spectrum, with good efficiencies and line widths as well as device lifetimes.

Photoluminescent dye dopants have been incorporated into a variety of different OLED structures and materials. PL dyes have been incorporated into both the hole transporting layer (HTL) and the electron transporting layer (ETL) of single heterostructure devices, as well as the emissive layer of double heterostructure OLED's. In addition to these multilayer structures, PL dye dopants have been used very effectively in single-layer devices, which are built from blends of hole and electron transporting polymers or molecular materials. The role of the dye in controlling the EL spectrum and the processes that are involved in energy transfer to the dye are the same whether a small molecule or polymer based device is being discussed. We will use examples from both small molecule and polymer based OLED's interchangeably throughout this article.

In addition to efficient color tuning there are a number of other benefits of dye doping into OLED's. If the dye is well matched to the material it is codeposited with, the EL output from this device will come exclusively from the dye dopant, even at very low dye-loading levels [6], [11], [12]. The dye traps the excitons formed in the device and subsequently emits. By shifting the emission from the HTL or ETL to the dye, the efficiency of the device can be improved significantly. This increase in quantum efficiency is due largely to the improved luminescence efficiency of the dispersed dye relative to the dense ETL or HTL that it is doped into. In addition to improving the luminescence quantum efficiencies of OLED's, dye doping can enhance the probability for hole–electron recombination, leading to substantial improvements in power efficiency [9], [10], [13]. Another benefit of dye doping on the EL output is that dye-doped devices often give significantly narrower EL spectra than nondoped devices. This is a tremendous advantage in full color display applications, which involve mixing of red, green, and blue light at each pixel to generate the various colors of the spectrum. In order to create saturated colors it is important for the individual red, green, and blue lines to be as narrow as possible. If the lines are broad, substantially unsaturated or washed out colors will result. Dye doping can also lead to significant enhancements in the stability of the OLED [14], preventing crystallization of the glassy HTL or
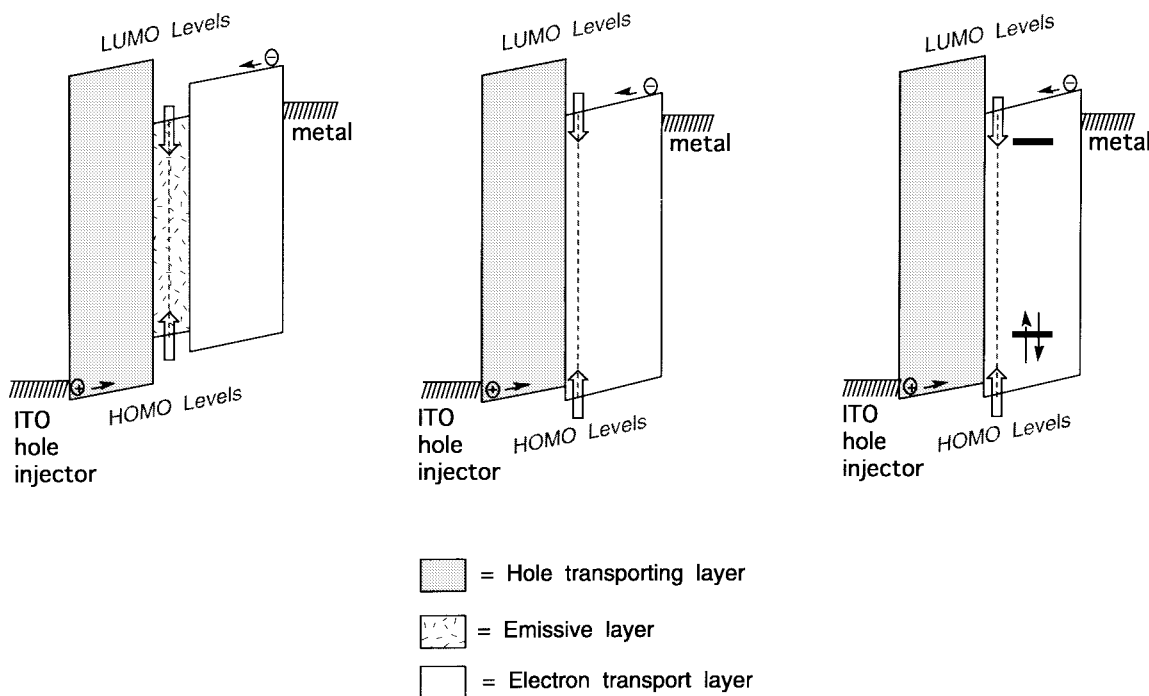
Fig. 1. Typical band structure diagrams for a double heterostructure OLED (left), a single-heterostructure OLED (center), and a PL dye-doped single-heterostructure OLED (right). The double arrows tied by a dashed line represent the correlated hole–electron pairs of the Frenkel excitons formed in the devices. The dye is represented by the HOMO and LUMO levels in the ETL.

ETL materials. This glass stability and other factors lead to longer device lifetimes for these doped devices, compared to the undoped analogs.

In this paper, we will discuss the important parameters in choosing a good dye dopant for a given OLED structure. The process of energy transfer to the dye in these devices will be discussed as well as the use of dye doping to probe mechanistic issues in these multilayer devices. We will focus on the properties of these devices including their construction, efficiencies, color purity, and chromaticities.

II. LUMINESCENT DOPANTS IN OLED'S

In an OLED a number of different criteria need to be satisfied to have a high probability for electron and hole radiative recombination. In order to balance the injection of holes and electrons into the organic materials and improve the likelihood of hole–electron recombination within the organic materials in these devices, multiple organic layers are typically used with each layer optimized for its particular role as a carrier injector or light emitter [7]–[10]. Both double heterostructure OLED's (HTL/emitter/ETL) and single-heterostructure (HTL/ETL) OLED's have been fabricated and can have very good electron $\rightarrow$ photon quantum efficiencies [15, pp. 593, 633]–[18]. Schematic band diagrams for these two types of OLED are shown in Fig. 1. In this device, the preferred conductivity of holes in the HTL and electrons in the ETL leads to a build up of carriers at the HTL/ETL interface, as in the double heterostructure. In these OLED's, the hole–electron recombination occurs at or near the HTL–ETL interface to form a Frenkel exciton. This Frenkel exciton is illustrated by the sets of linked arrows in Fig. 1. The exciton will be trapped in the material with the lowest exciton energy (E_{ex}), but free to migrate within that layer [19]. The most common situation is for the exciton to be trapped in the ETL $[E_{ex}(\text{ETL}) < E_{ex}(\text{HTL})]$. The exciton diffuses randomly through the matrix until it decays, either radiatively or nonradiatively. The emission from the OLED comes from the same excitonic state that would be formed by photoexcitation.

The first efficient EL device was a single heterostructure, with a tertiary amine HTL and an aluminum complex (Alq_3) serving both as the ETL and emitter [5]. In this device, the preferred conductivity of holes in the HTL and electrons in the ETL leads to a build up of carriers at the HTL/ETL interface, as in the double heterostructure. The excitons are formed at the interface and are not spatially confined. As a result, it is important that the thickness of the ETL/EM layer be chosen such that the majority of the excitons decay before they migrate to the electrode, where they will be quenched. The problem of exciton diffusion in the organic materials can be solved by moving to a double heterostructure device. In a double-heterostructure OLED, an emissive (EM) layer is inserted between the HTL and ETL. This EM layer is chosen so that it has a lower exciton energy than either the HTL or ETL, leading to efficient trapping of excitons in the EM layer. In addition, the highest occupied molecular orbital (HOMO) of the EM is at a higher energy than that of the HTL, and its lowest unoccupied molecular orbital (LUMO) is lower in energy than that of the ETL, thus both holes and electrons can be efficiently transferred to and trapped in the EM layer.

The picture presented above for efficient confinement of the excitons within the device is based on an EM layer sandwiched between the HTL and ETL. The EM does not need to be a discrete layer in the OLED, however, for exciton confinement
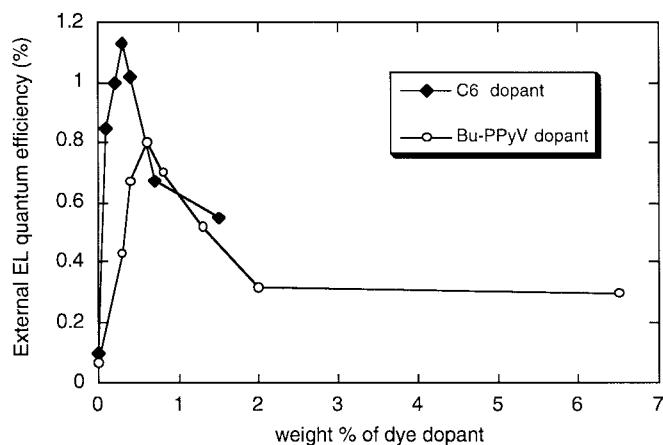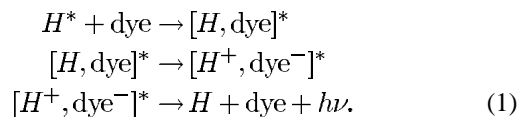
Fig. 2. Plot of dye doping level versus OLED quantum efficiency. The PL dopants in this example are Coumarin 6 (C6) and a low-molecular weight polymer (polypyridylvinylene), the host matrix is polyvinylcarbazole [16].

to occur. A PL dye-doped into the HTL or ETL can also act as an emissive trap, in the same way the EM layer does in the double heterostructure OLED. As long as the exciton energy (E_{ex}) of the host is greater than the absorption energy of the dye dopant, excitons will be effectively trapped or confined on the dopant molecules leading to improved EL efficiency. A schematic representation of the band structure in a dye-doped OLED is shown in Fig. 1. Just as one observes in a double heterostructure, the excitons are trapped within the organic material (on the dye), and hence can not diffuse to the electrode where they would be quenched. In addition, since the dye molecules are isolated, their luminescent efficiencies can be significantly greater than the ETL or HTL materials. The luminescent yields (as measured by PL) for isolated organic molecules can be close to 1, while the efficiencies for the thin film ETL and HTL materials (Alq_3 and TPD, respectively) are less than 0.35 [20]. Keeping the dye dopant in low concentration in the OLED is very important, since the same dyes as pure materials give PL efficiencies typically very poor. A plot of the EL and PL quantum efficiencies as a function of the dye loading level is shown in Fig. 2 [16]. A peak in efficiency is observed at just under 1% dye loading for both of the dyes investigated here. Above this level the dye begins to aggregate, leading to extensive self-quenching and luminescence losses. The self-quenching process often involves formation of nonemissive excimer states. In an excimer, the exciton is delocalized over two molecules, i.e., $A^* + A \rightarrow A_2^*$ (A_2^* = excimer). The excimer can luminesce, but typically does so with a low quantum efficiency [26]. The dimer formed in the excimeric state is not bound in the ground state and dissociates to monomers on relaxation from the excited state.
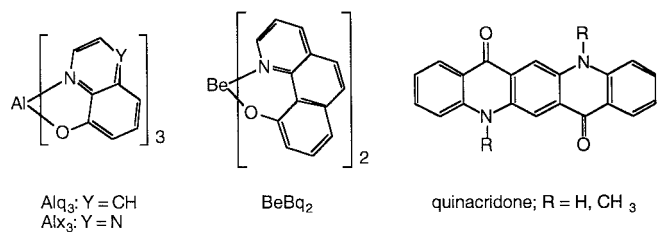
The formation of excimer states at high dye loading levels has two negative consequences, the emission band is broad and the quantum efficiency for luminescence is low. A related process can occur even at low dye-loading levels, in which an excited dimer state is formed between the dye and a molecule of the host matrix. The dye/host dimer is called an exciplex and results from electron transfer from one molecule to the other. The process is illustrated in (1), where H^* is the host bound

exciton, $[H, \text{dye}]$ is an encounter complex and $[H^+, \text{dye}^-]^*$ is the exciplex. This process is illustrated for electron transfer from the host to the dye, but it could also be the case that electron transfer occurs from the dye to the host. Like the excimer, the exciplex is only bound in the excited state, i.e., there is no donor–acceptor complex in the ground state. The first report of exciplex states in OLED's involved an exciplex formed at the HTL/ETL interface [21]:

$$H^* + \text{dye} \rightarrow [H, \text{dye}]^*$$
$$[H, \text{dye}]^* \rightarrow [H^+, \text{dye}^-]^*$$
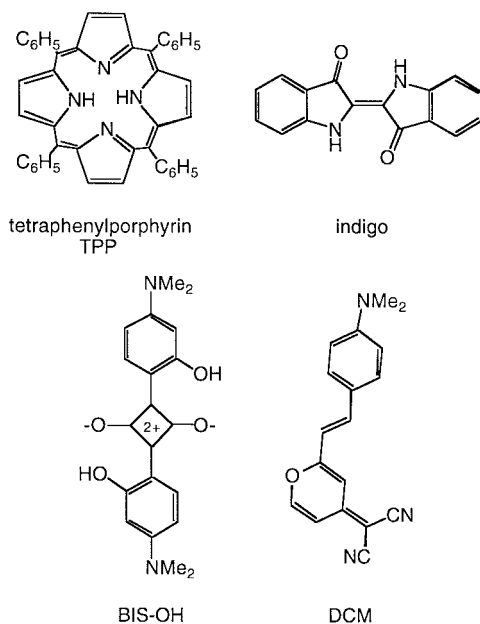$$[H^+, \text{dye}^-]^* \rightarrow H + \text{dye} + h\nu. \tag{1}$$

In addition to effecting the electrical properties and color of OLED spectra, dye doping can significantly enhance device lifetimes. Tang *et al.* [6] demonstrated that by doping aluminum tris(8-hydroxyquinolate) (Alq_3) with laser dyes, the OLED lifetime could be improved relative to undoped devices. The doping of ETL and HTL layers of molecular organic devices with rubrene has been examined and showed an influence of the doping site location on the stability of the devices [13]. $BeBq_2$ based devices give very high luminance ($> 10\,000$ cd/m^2) and luminous efficiency [22]. Devices were prepared with a thin tertiary amine hole injecting layer (MTDTA) and tested with an initial luminance of 500 cd/m^2, leading to the conclusion that for TPD/$BeBq_2$ OLED's the preferred site for doping is the HTL. A reference (undoped) device (ITO/MTDTA/TPD/$BeBq_2$/Mg–In) gave a half-life ($T_{1/2}$) of only 23 h. When rubrene was doped into the HTL the OLED gave a $T_{1/2}$ of 3554 h, while a device with the rubrene doped into the ETL gave a $T_{1/2}$ of 110 h. Both of these doped devices had a longer lifetime than the reference device, but the doped HTL structure is best. For comparison an analogous Alq_3 based device (ITO/MTDTA/TPD/Alq_3/Mg–In) gave a $T_{1/2}$ of 1150 h. The authors site control of the location of carrier recombination as the primary reason for the enhanced lifetimes in the TPD-doped OLED's.

The importance of using the appropriate host-dopant system was showed in another study, in which Alq_3-based devices doped with different quinacridone derivatives were prepared and their lifetimes measured [9], [10]. For the undoped Alq_3 OLED, the half-life time was about 4000 h, operating from an initial luminance of 510 cd/m^2. The lifetime of the Alq_3 device doped with quinacridone (Scheme 1, R = H) was decreased by a factor of 10. When methyl substituted derivative of quinacridone (Scheme 1, R = CH$_3$) was doped into an otherwise identical Alq_3 device, the half-life increased to more than 6000 h with an initial luminance of 1400 cd/m^2. The luminance efficiency of this long-lived device is nearly triple that of the undoped device (at comparable luminance levels). Device lifetimes are closely related to the number of coulombs of charge that are passed through the device, i.e., high-current levels lead to a short lifetimes [9], [10], [23]. Since the light output and current level are proportional, the $T_{1/2}$ value for a given device is dependent on luminance level that is produced. If an OLED is run at a 100 cd/m^2 (the brightness of an average CRT) rather than 1400 cd/m^2, the 6000 h $T_{1/2}$ is expected to increase to $>50\,000$ h. Close examination of a rubrene doped

Alq$_3$: Y = CH
Alx$_3$: Y = N

BeBq$_2$

quinacridone; R = H, CH$_3$

Scheme 1.

Matrix Materials

BAlq

DPVBi

PBD

PVK

BSA-2

PS

TPD

tetraphenylporphyrin
TPP

indigo

BIS-OH

DCM

Scheme 2.

Dopants

rubrene

BPEA

M = Eu, Eu(MeOBB)$_3$
Tb, Tb(MeOBB)$_3$

BCzVB   Ar =

BCzVBi   Ar =

Nile Red

Eu(DBM)$_3$(Phen)

Bu-PPyV

Anthracene

Perylene

TPB

C6 (C540)

C47

C510

Ph9

DCM1

DCJT

BIS-OH

Indigo

t-BuPh-PTC

Sq

TPP

JF3

Scheme 3.

Alq$_3$ film shows that the rubrene doping stabilizes the Alq$_3$ toward recrystallizaton or morphological change at elevated temperatures (73 °C in vacuo) [14]. An undoped Alq$_3$ film examined under the same conditions completely deteriorated. The higher stability of the doped devices is related to several factors. The higher luminance efficiency of the dye-doped devices is expected to improve the lifetime, since the device does not need to driven as hard to achieve the same brightness as an undoped device. Other factors such as suppression of crystallization and control of the site and energetics of carrier recombination also contribute to the improved OLED lifetimes for doped devices.

III. ENERGY TRANSFER IN DYE-DOPED OLED'S

There are a number of different processes that can occur in dye-doped OLED's which will lead to exciton trapping at the dye. The most simple process, often referred to as trivial energy transfer, involves emission from the donor (e.g., Alq$_3$), reabsorption of the photons by the dye and finally emission from the dye. While this process can be efficient for very optically dense samples, it is not practical for OLED's. The organic films themselves must be very thin (<500 Å per layer) for the devices to function. At this thickness, it is not possible to have enough dye present to absorb a reasonable amount of the light, without going to doping levels so high that the dye would self-quench and degrade device performance.
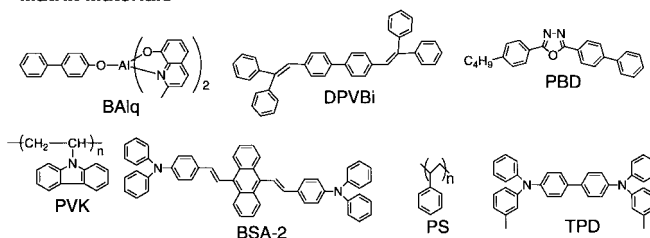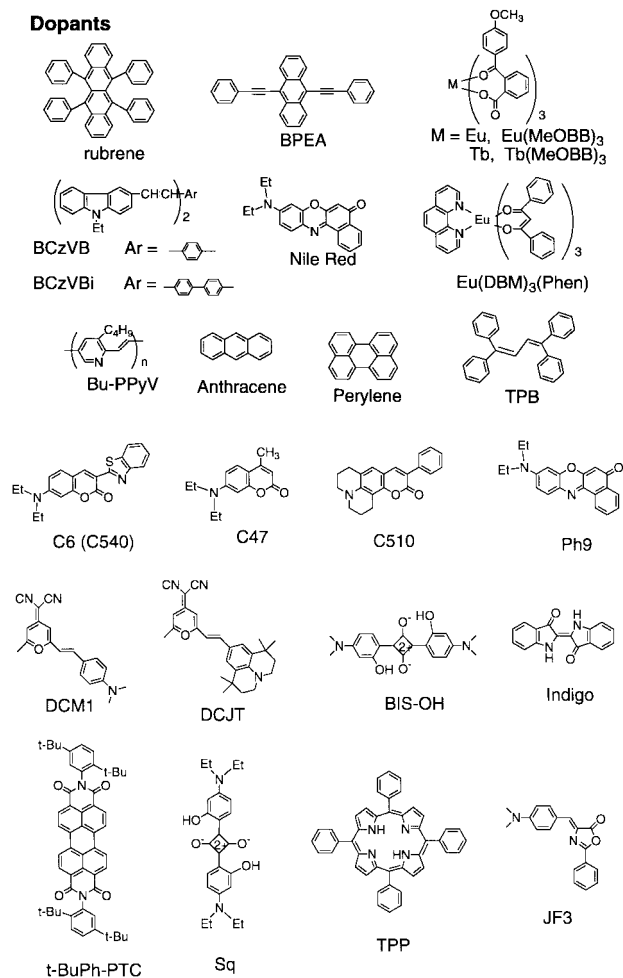
For example, tetraphenylporphyrin (TPP) has a fairly high-extinction coefficient ($\varepsilon_{516\,nm} = 2.3 \times 10^4$ M^{-1} cm^{-1}), and when doped at 1% in Alq$_3$ gives a film with an optical density for the TPP of less than 0.05. At this optical density less than 10% of the Alq$_3$ emission would be absorbed and reemitted by TPP. The result would be an OLED with an emission spectrum barely changed from Alq$_3$. At this doping level, however, an Alq$_3$ OLED doped with TPP gives emission exclusively from the TPP dopants [45], indicating that other processes must be considered in understanding PL dye-doped OLED's.

Clearly, other mechanisms beside the trivial energy transfer mechanism must be active in PL dye-doped OLED's. The dominant processes involve both exciton and carrier trapping by the dye dopants. An exciton is formed near the HTL/ETL interface in the OLED and diffuses through the medium until it encounters a dye molecule. If the dye has a lower energy
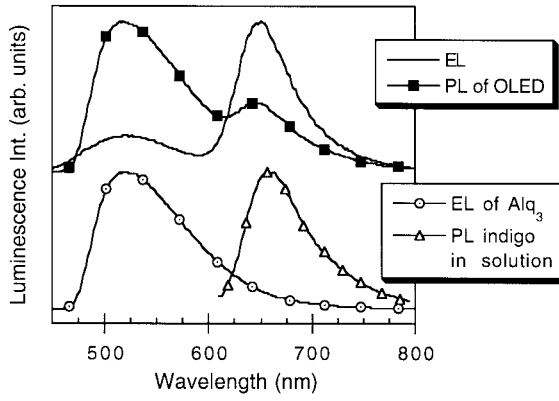
Fig. 3. PL and EL spectra of an OLED prepared with an indigo doped Alq$_3$ ETL. For comparison the EL spectrum of Alq$_3$ and the PL spectrum of indigo in methylene chloride are shown.

absorption than E_{ex} of the HTL or ETL, energy transfer to the dye will be favorable. There are two different mechanisms that can be active for this energy transfer. The first is facilitated by a Coulombic interaction between the HTL or ETL bound exciton and the PL dye, and is referred to as Förster energy transfer. The second mechanism for energy transfer involves an electron–exchange interaction between the exciton and the PL dye, and is referred to as Dexter energy transfer. We will discuss both of these energy transfer processes below. An independent process for exciting the dye molecules involves carrier trapping [24]. In this process the dye acts as a trap for either holes or electrons. When current is passed through the device, one of the carriers (hole or electron) is trapped at the dye and eventually recombines with the opposite carrier, forming the dye bound exciton. This carrier trapping process is very common and can occur in parallel with energy transfer in a given device. The only requirement for efficient carrier trapping is that the dye dopant must have a HOMO energy higher than the HOMO of matrix it is doped into or a LUMO energy lower than that of the matrix material.

The relative contributions of the dye dopant and the matrix (HTL or ETL) to the PL spectrum of the doped thin film is only governed by energy transfer processes, since photoexcitation of the thin film does not generally lead to free carriers. In the EL spectrum, however, both carrier trapping and energy transfer can contribute to dopant emission. By comparing the two spectra, it may be possible to determine if carrier trapping or energy transfer is more important in EL. An example of such a study is shown in Fig. 3. The device used in this study had 0.7 mol % of indigo doped into the Alq$_3$ layer of an ITO\TPD\Alq$_3$–indigo\Mg–Ag OLED [11]. The EL spectrum from the device is very similar to the PL spectrum of the free dye in solution, consistent with dominant emission from the dye dopant. The PL spectrum of the dye-doped thin film, on the other hand, has a large amount of emission from Alq$_3$ in addition to emission from indigo. Clearly, some degree of energy transfer is occurring from Alq$_3$ to the dye to give rise to the small amount of dye based emission observed in the PL spectrum, but the fact that the EL spectrum shows dominant emission from the dye is due to both energy transfer and carrier trapping processes working together in the device.

Förster energy transfer can be a very efficient process for transferring energy from an HTL or ETL bound exciton to a PL dye dopant [25], [26]. For the purposes of this discussion and the following discussion of Dexter energy transfer, we will define the ETL or HTL molecule as the donor (of energy) and the dye dopant as the acceptor (of energy). Förster energy transfer involves a dipole–dipole coupling of the transition dipole moments for excited donor (exciton) and the dye in its ground state. As the excited donor relaxes, its energy is transferred via a strong Coulombic interaction with the dye molecule, Fig. 4(a). The advantage of this sort of energy transfer process is that the dipole–dipole interaction can be quite strong over large distances, allowing efficient energy transfer over distances of up to 100 Å in very favorable cases. In order to assess the efficiency of such a process it would be useful to be able to evaluate the rate of energy transfer relative to radiative relaxation of the donor (e.g., Alq$_3$ exciton). A high rate of energy transfer relative to radiative relaxation will lead to emission exclusively from the dye dopant. An analytical expression for the rate of Förster energy transfer (dP_n/dt) has been derived, and is given in (2a). In this equation, κ^2 is an orientation factor, which has a value of 2/3 for random donor–acceptor orientations as found in doped OLED's, n is the refractive index of the medium ($n = 1.7$ for Alq$_3$) [20], NA is Avagardro's number, r is the donor acceptor separation and τ_D is the fluorescent lifetime of the donor. $F_D(\tilde{\nu})$ is the fluorescence spectrum of the donor, defined as in (2c), where Φ_{PL} is the fluorescence quantum yield, $\varepsilon_A(\tilde{\nu})$ is the molar decadic extinction coefficient spectrum of the acceptor, and $\tilde{\nu}$ is the energy in wavenumbers. The integral in (2a) measures the degree of spectral overlap between the donor PL and acceptor absorption spectra, Fig. 4(b). A high degree of overlap favors a high rate of energy transfer. Unfortunately, it is difficult to apply this equation to randomly doped systems, such as those used in OLED's. The problem arises from the fact that the dipole–dipole interaction and, thus, the energy transfer will have a strong distance dependence. The broad distribution of distances in the randomly doped sample would lead to a broad distribution of rates. A more common approach to evaluating Förster energy transfer is to calculate the Förster radius R_0 given in (2b) [26], [27]. The Förster radius is defined as the distance between the donor and acceptor at which the probability of intermolecular energy transfer equals that of relaxation of the donor by fluorescence or unimolecular processes. A large Förster radius is indicative of a very efficient energy transfer process, which will compete with unimolecular relaxation very effectively at distances shorter than R_0. A short Förster radius is indicative of a very inefficient process that requires very short donor–acceptor distances to be effective:

$$\frac{d}{dt}P_n = \frac{0.5291\kappa^2}{n^4 N_a r^6 \tau_D} \int_0^\infty F_D(\tilde{\nu})\varepsilon_A(\tilde{\nu})\frac{d\tilde{\nu}}{\tilde{\nu}^4} \qquad (2a)$$

$$R_0^6 = \frac{0.5291\kappa^2}{n^4 N_a} \int_0^\infty F_D(\tilde{\nu})\varepsilon_A(\tilde{\nu})\frac{d\tilde{\nu}}{\tilde{\nu}^4} \qquad (2b)$$

$$\Phi_{PL} = \int_0^\infty F_D(\tilde{\nu})\, d\tilde{\nu}. \qquad (2c)$$

TABLE I

FÖRSTER RADII FOR A SERIES OF DONORS AND ACCEPTORS USED IN OLED'S. SEE SCHEME FOR DESCRIPTIONS OF COMPOUNDS

Extinction coefficient, $mol^{-1}dm^3cm^{-1}$, (λ_{max}, solvent)	Acceptor (dye dopant)	Donor (Host)	R_0 (Å)
9.3×10^4 (618nm, DMSO)	Indigo	Alq_3	29
"	"	Alx_3	16
840 (538nm, toluene)	C_{60}	Alq_3	22
3.0×10^4 (634nm, DMSO)	BIS-OH	Alq_3	37
"	BIS-OH	Alx_3	21
2.3×10^4 (516 nm, toluene)	Tetraphenylporphyrin	Alq_3	33
1.0×10^5 (530nm, EtOH)	Rhodamine 6G	Alq_3	41
4.4×10^4 (461nm, toluene)	DCM	Alq_3	33

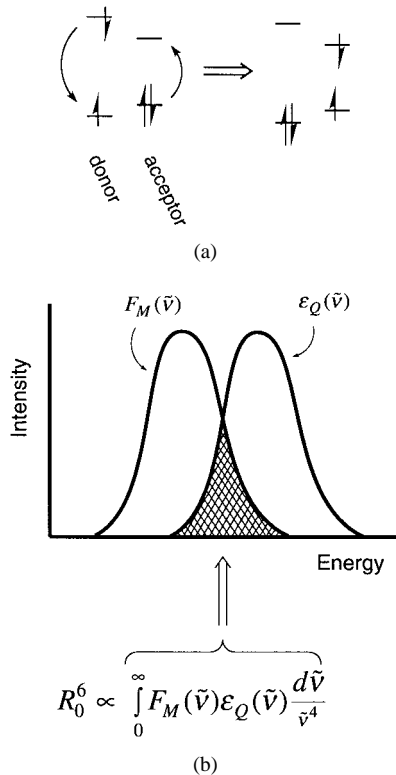$$R_0^6 \propto \int_0^\infty F_M(\tilde{v})\varepsilon_Q(\tilde{v})\frac{d\tilde{v}}{\tilde{v}^4}$$

(b)

Fig. 4. (a) Schematic representation of Förster energy transfer. (b) Overlap integral from (2) shown as the shaded region of the curves.

Fig. 5. Absorption spectra of TPP and DCM, plotted with the EL spectrum of Alq_3.

A number of different dopants have been used in Alq_3 based OLED's. The absorption spectra of two different dopants (DCM and TPP, see Scheme 2) along with the luminescence spectrum of Alq_3 are shown in Fig. 5. Both of these dopants have large extinction coefficients and good overlap with the Alq_3 luminescence spectrum. The Förster radii for energy transfer from Alq_3 to these dopants and several others are given in Table I. Most of the radii calculated for these materials are larger than 30 Å, indicative of very favorable energy transfer processes. An aluminum tris(5-hydroxyquinoxaline) host (Alx_3) [11], however, gives relatively short Förster radii. The reason for the short radii in Alx_3 is not related to spectral
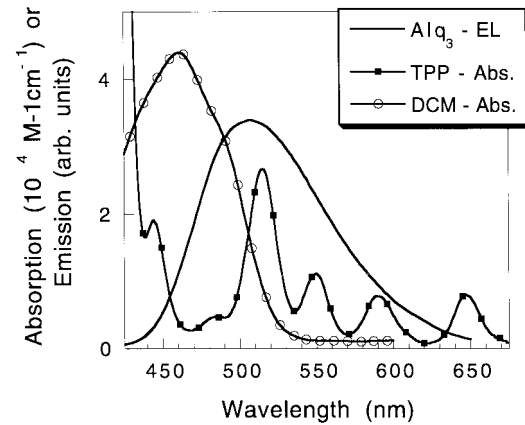
overlap, but to a low PL efficiency for the host matrix [11]. The PL efficiency for Alx_3 is roughly 100 times less than that of Alq_3, which leads to a decrease in R_0 by a factor of 2. Energy transfer from Alq_3 to C_{60} also results in a comparatively short R_0 of 22 Å. The spectral overlap between Alq_3 PL and C_{60} abs spectra are excellent, but the extinction coefficient for C_{60} is low leading to a relatively short R_0. Thus, for achieving large Förster radii, it is important to have a donor with a high Φ_{PL} (e.g., $\Phi_{PL}(Alq_3) = 0.32$ [20]) and an acceptor with a high ε_A, in addition to significant spectral overlap.

It is valuable to consider the impact that this radius has on the optimal doping level in dye-doped OLED's. At too high a doping level the dye molecules self quench their own emission leading to low quantum yields, and at too low a dye concentration there will not be enough dye to trap the electrically generated excitons before they relax. The optimal concentration of dye dopant in OLED's has been found to be typically below 5 mol%. This number is easy to understand if we compare the average dye–dye distance and the Förster radius. Assuming the dyes are uniformly dispersed in the Alq_3 matrix, a dye doping level of 1% would correspond a sphere of 100 Alq_3 surrounding each dye molecule, with a radius of roughly 3 Alq_3 molecules $(4\pi r^3/3 = 100)$. The diameter of

Alq$_3$ is roughly 9 Å, leading to an estimate of 27 Å for the maximum distance that an Alq$_3$ exciton can be from a dopant molecule. This value is close to or below the Förster energy transfer radius for most of the dyes in Table I. The situation improves further when exciton migration is taken into account. An exciton that is formed near or outside of the Förster radius to the nearest dye molecule can readily migrate to a position that is within the Förster radius, promoting energy transfer prior to relaxation. The distance the exciton can migrate can be several times larger than the Förster radius. For Alq$_3$, for example, the exciton can migrate more than 200 Å prior to relaxation [6], [28].

The Förster energy transfer process described above relies on strong dipolar coupling to facilitate long distance energy transfer. An alternative process for energy transfer may also be active in dye-doped materials, which achieves energy transfer via an electron exchange mechanism. This process is often referred to as Dexter energy transfer and is shown schematically in Fig. 6 [25], [29].[1] Either simultaneous or consecutive electron transfers lead to the donor in its ground state and the acceptor in its electronic excited state. This transfer mechanism can be visualized as occurring by formation of a transient exciplex, which relaxes to a ground state on the donor and an excited state on the acceptor. The rate of Dexter energy transfer (dP_n/dt) is proportional to the degree of overlap between the donor emission spectrum (E_D) and the acceptor absorption spectrum (A_A), (3) [29]. Contrary to the case found for Förster energy transfer, however, the emission and absorption spectra are normalized, removing any dependence of the rate on the donor PL efficiency or the acceptor extinction coefficient. The integral of (3) is normalized such that complete overlap of the emission and absorption spectra corresponds to value of 1.00 [25], [29]. The parameter Z can not be obtained directly from optical experiments, but is related to the electronic matrix element for electron–exchange energy transfer. The magnitude of Z is dependent on the donor–acceptor distance, as shown in (3), where r is the donor–acceptor distance and L is the sum of the van der Waals radii of the donor and acceptor molecules. Dexter energy transfer is fastest for very short donor–acceptor separations and decreases rapidly as the separation increases. The rate of energy transfer by a Dexter type mechanism is expected to drop to negligible levels beyond a 15–20 Å donor–acceptor distance in Alq$_3$ [29]. Dexter energy transfer can be significantly faster than Förster transfer when either the donor or acceptor is not in a singlet state. Förster energy transfer requires that both the donor and the acceptor be singlets. Dexter energy transfer, however, does not have a singlet requirement and can efficiently act to transfer energy between triplet states or between singlet and triplet states [25], [30]. It is often difficult to predict which energy transfer mechanism will be dominant for a particular donor–acceptor separation. There is no question that at large distances Förster transfer is the only option, since the Dexter mechanism will require electron transfer, which would be very slow at large
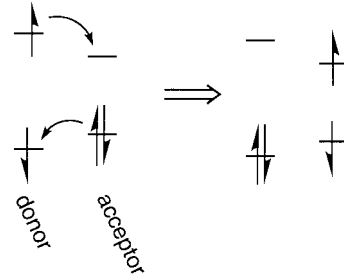
[1]The electron–exchange energy transfer rate is expected to drop to negegible levels for a given site beyond a sphere containing 40 lattice sites [29]. This is a sphere of radius 2.1 molecules, which corresponds to roughly 18 Å for Alq$_3$.

Fig. 6. Dexter electron–exchange energy transfer process.

distances:

$$\frac{d}{dt}P_n = \frac{2\pi}{\hbar}Z^2 \int_0^\infty E_D(\tilde{\nu})A_A(\tilde{\nu})\,d\tilde{\nu}, \qquad Z^2 \propto e^{-2r/L}. \quad (3)$$

The discussion thus far has centered on intermolecular energy transfer, however, in some OLED's intramolecular energy transfer is very important. Both Eu and Tb complexes have been used to make OLED's [31]–[34]. Examples of the complexes used in these devices are shown in Scheme 3. The OLED's in these lanthanide ion based devices are designed to emit in the green or red. These high energy excitons are transferred to the ligands of the lanthanide complex, as described above, and the energy is transferred to the metal ion. The EL spectra from these devices consist of very narrow lines and are identical to the atomic emission spectra of the same ions. The dominant transitions for the Tb ion are $^5D_4 \rightarrow {}^7F_6$ and $^5D_4 \rightarrow {}^7F_5$, while those of the Eu complex are $^5D_0 \rightarrow {}^7F_1$ and $^5D_0 \rightarrow {}^7F_2$. The Tb complex gives green EL (two lines are observed at $\lambda_{\max} = 490$ and 545 nm), and the Eu complex gives red EL (two lines at $\lambda_{\max} = 585$ and 617 nm). While this approach leads to very narrow lines and good chromaticity (*vide infra*), the efficiencies of the reported devices are less than many dye-doped devices (the maximum brightness of 460 cd/m^2 at a drive voltage of 16 V was reported for the Eu complex based device [33] and 45 cd/m^2 at 24 V for the Tb complex device [31]). The low efficiencies of the lanthanide based devices are related to their low-energy transfer efficiencies. The energy transfer process in these materials can be understood in terms of two energy transfer processes necessary for the emission of the lanthanide ion in the device. During this two-step energy transfer, several nonradiative deactivation processes can occur: 1) at the ligand levels prior to the energy transfer from the ligand to the ion; 2) within the manifold of rare-earth upper levels; and 3) at the emitting level of the ion [35]. For example, in certain terbium chelates quenching of the emitting level of the ion by the ligand triplet (in solution) is a strong deactivation pathway [35]. Consequently, the overall energy loss in this case is more pronounced than that in the case involving only a simple energy transfer from the host molecule to the organic dye.

IV. CHROMATICITY OF DYE-DOPED OLED'S

In order to determine how the light output of one OLED compares to another with regards to color and saturation it is important to have a quantitative means of assessing these values. The system that is commonly used to evaluate OLED's

(as well as CRT's and other emissive displays) is the CIE system (CIE = Commision Internationalde l'Eclairage) [36], [37]. The CIE is based on the stimuli generated in the human eye by visible light. There are three different types of cone cell in the eye, responsible for color discrimination, with their absorption maxima centered at 419, 531, and 558 nm [38]. If the sensitivity functions for the three cones are summed, one obtains the photopic response, which is centered in the green (at 505 nm), and falls off steeply toward the blue and red. The CIE system is based on the fact that any pure (monochromatic) color can be visually matched by an additive mixture of red, green and blue light in the appropriate proportions. Through color matching experiments, the required amounts of red, green and blue primaries needed to match a light of arbitrary wavelength were determined. These experiments have led to a set of response functions for color matching, $\overline{X}$ (red), $\overline{Y}$ (green) and $\overline{Z}$ (blue), where $\overline{Y}$ corresponds exactly with the photopic response function. Using these functions a given emission spectrum can be converted into a set of three tristimulus values ($X, Y,$ and Z) that uniquely define the color and degree of saturation that will be perceived for that emission source.

In order to represent the tristimulus values on a two dimensional plot, $X, Y,$ and Z are converted to their fractional contributions [i.e., $x = X/(X+Y+Z), y = Y/(X+Y+Z)$ and $z = Z/(X+Y+Z)$]. A plot of x versus y is used to visualize how the colors are organized by the CIE system. This plot is termed the CIE chromaticity diagram, and is shown in Fig. 7. Monochromatic colors fall on the perimeter of the horseshoe shaped curve starting with blue in the lower left, running through the colors of the spectrum in a clockwise direction to red in the lower right. The colors along the line at the bottom are not pure colors, but would be made by color mixing. White or the neutral point is found at the center of the diagram, labeled W. As a given point is moved toward the white point from the perimeter the color remains constant, but progressively more unsaturated. Using the CIE diagram it is easy to see how two parameters can be defined for a given x, y point. The dominant wavelength (λ_D) is defined by the intersection point of a ray connecting the white point and x, y with the monochromatic (or saturated) color perimeter of the CIE, see Fig. 7. A second parameter for a given point x, y is the purity of the color, p_e. The color purity is defined as the ratio of the distance between the white point and x, y to the distance between the white point and λ_D (i.e., $|(x, y - W)/(\lambda_D - W)|$, a/b in Fig. 7). A saturated or monochromatic light source will have a p_e of 1 and very unsaturated color will have a small p_e value.

By mixing the outputs of saturated red and green light sources in different ratios it is possible to generate all of the colors along the right side of the horseshoe of the CIE diagram. If a blue source is added to the mixture, any of the colors within the triangle defined by the x, y coordinates of the three points can be prepared. For reference, the CIE coordinates of the red, green and blue phosphors used in CRT's (Natioanl Television Systems Committee, NTSC, U.S. and Japan) are shown in Fig. 8 [39]. High-p_e values for the individual points are very important in full color display applications, since the
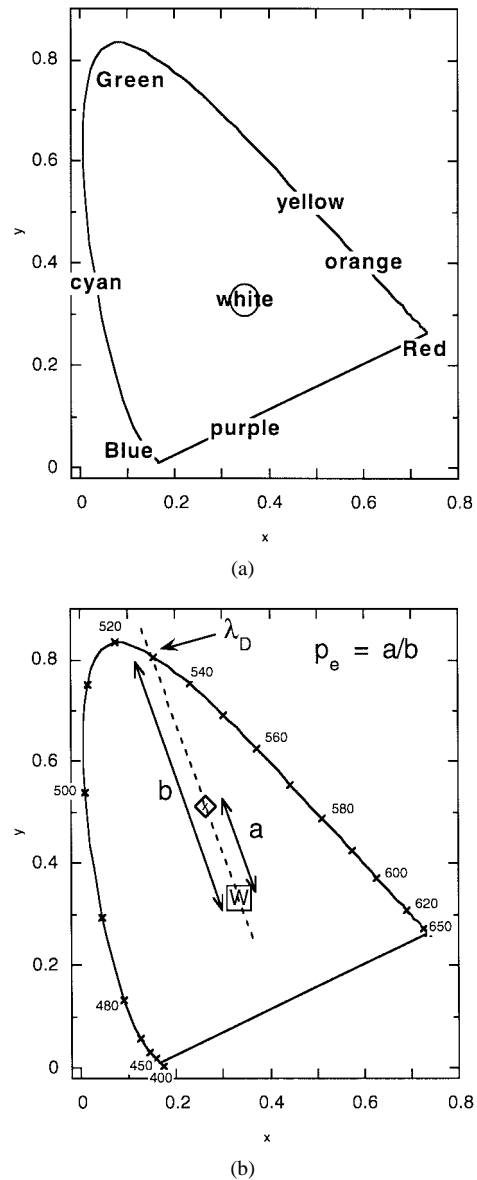

Fig. 7. CIE chromaticity diagram. (a) The CIE coordinates of all visible colors fall within the curve. Approximate positions of the saturated colors are labeled. (b) Positions of saturated colors are shown as crosses on the perimeter of the CIE diagram. The coordinates of the point used for illustration of $\lambda\delta$ and p_e (labeled with an x) are those for an undoped Alq$_3$ based OLED. The white point (labeled w) in the center of the plot is obtained by summing equal amounts of red, green, and blue.

p_e values of the sources limit the accessible p_e values for the mixtures. In order for OLED's to be used in full-color display applications, it will be important for their EL spectra to correspond to red, green, and blue spectral regions, with high-p_e values. A number of dye-doped OLED's have been reported with colors spanning the entire visible spectrum. Table II lists the dye, matrix doped, CIE coordinates, λ_D and p_e values for a number of dye-doped OLED's. The CIE coordinates for each of these devices are plotted in Fig. 8. The plots clearly illustrate that most of the OLED's reported give substantially unsaturated emission. Dye doping does lead to significant line narrowing relative to the undoped OLED, however, the degree of line narrowing is not sufficient in many cases to achieve saturated emission. Several promising candidates do show up,

TABLE II
CHROMATICITY COORDINATES FOR A VARIETY OF DYE-DOPED OLED'S. THE IDENTITIES OF THE DYE DOPANTS
ARE GIVEN IN SCHEMES 1–3 AND THE DEFINITION OF THE TERMS LISTED ARE DESCRIBED IN THE TEXT

#	Dye Dopant	Matrix Doped	CIE Coordinates	λ_D (nm)	P_e	ref.
1	TPB, C6, DCM1	PVK	0.27 , 0.39	white	0.28	40
2	C47	PVK, PBD	0.16 , 0.10	462	0.84	16
3	perylene	BAlq	0.16 , 0.19	480	0.70	9
4	BCzVB(i)	DPVBi	0.14 , 0.21	483	0.73	42
5	C510	PS	0.20 , 0.34	493	0.43	12
6	C6	PVK, PBD	0.23 , 0.53	520	0.40	16
7	JF3	Alq$_3$	0.26 , 0.57	533	0.51	46
8	Tb(MeOBB)$_3$	PVK, PBD	0.26 , 0.57	533	0.51	31
9	C6	Alq$_3$	0.26 , 0.62	540	0.68	9
10	anthracene	Alq$_3$	0.28 , 0.57	541	0.59	43
11	C540 (C6)	Alq$_3$	0.27 , 0.65	543	0.79	6
12	C6	PS	0.29 , 0.65	546	0.85	44
13	BPEA (1.62%)	Alq$_3$	0.31 , 0.54	550	0.56	13
14	Bu-PPyV (0.5%)	PVK	0.32 , 0.52	551	0.53	16
15	t-BuPh-PTC	PS	0.36 , 0.51	561	0.64	12
16	DCM1	PS	0.39 , 0.59	564	0.94	12
17	Ph9	PS	0.43 , 0.51	570	0.83	12
18	rubrene	TPD	0.49 , 0.50	574	0.88	22
19	BPEA (14.5%)	Alq$_3$	0.47 , 0.51	575	0.92	13
20	rubrene	TPD	0.46 , 0.50	577	0.88	13
21	C60	Alq$_3$	0.40 , 0.39	578	0.33	11
22	BIS-OH	Alq$_3$	0.44 , 0.41	582	0.55	11
23	rubrene	Alq$_3$	0.53 , 0.47	583	1	13
24	BIS-OH	Alx$_3$	0.56 , 0.40	593	0.90	11
25	nile red	PVK, Alq$_3$	0.58 , 0.41	594	0.97	16
26	DCM1	Alq$_3$	0.60 , 0.40	595	1	6
27	Sq	BSA-2	0.61 , 0.39	597	1	24
28	DCJT	Alq$_3$	0.62 , 0.38	598	1	9
29	Eu(MeOBB)$_3$	PVK, PBD	0.53 , 0.36	602	0.65	31
30	Eu(DBM)$_3$(Phen)	PBD	0.65 , 0.35	612	1	33
31	indigo	Alx$_3$, or Alq$_3$	0.69 , 0.31	635	1	11
32	TPP	Alq$_3$	0.71 , 0.29	645	1	45

however, in the blue, green and red regions of the CIE (e.g., 2, 11, 12, 30, 31, 32 in Fig. 8), whose p_e values are close to 1 with λ_D values in the blue, green and red. Continued exploration of dyes and ETL or HTL host materials may lead to even more saturated red, green, and blue OLED's.

White light emission from single OLED's has been achieved by dye doping as well [40], [41]. Two different approaches have been used to prepare white OLED's. The first white OLED was prepared by doping three different dyes into the same polymer layer [40]. This device is point 1 in Fig. 8. Each dye in this device acts as an exciton trapping site and an independent emitting center, leading to an EL spectrum that is the sum of the three dye spectra. Careful control of the

doping levels for each dye was important, however, to prevent Förster energy transfer from the blue PL dye to the red and green PL dyes and from the green PL dye to the red PL dye. A multilayer stacked OLED has also been reported [41], which has dyes separated into different layers in a single OLED. In this device the blue and green emission come from TPD and Alq$_3$ layers, respectively, while the red emission comes from Nile Red doped Alq$_3$ film. The CIE coordinates for this white light-emitting device are $x = 0.34$, $y = 0.36$.

V. CONCLUSION

Dye doping into OLED's leads to a number of advantages over nondye-doped OLED's. Color tuning can be achieved
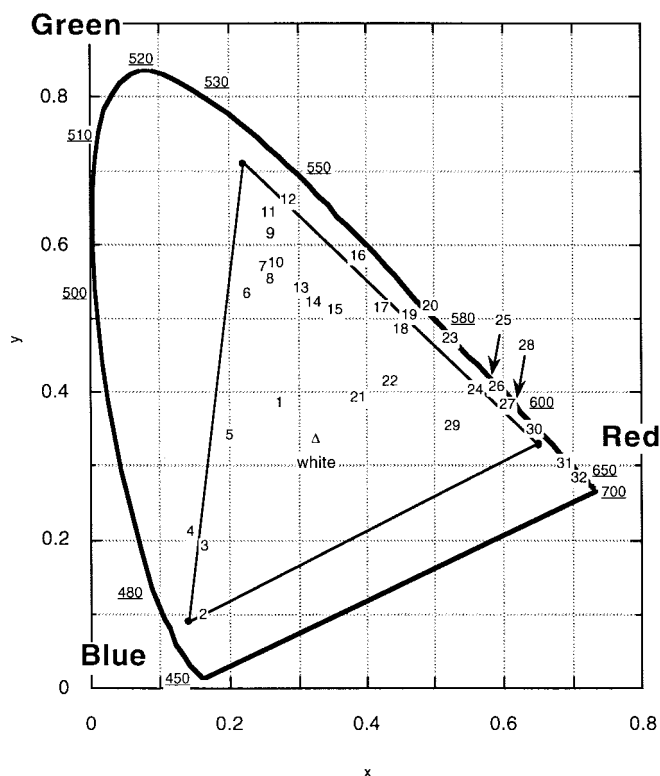
Fig. 8. Plots showing the CIE coordinates of the devices listed in Table II, The numbers correspond to the sample number in the table. Coordinates of monochromatic light sources are indicated by underlined numbers, corresponding to $\lambda\mu\alpha\xi$. The CIE coordinates for red, green, and blue NTSC CRT phosphors are shown by the triangle [39].

with improved quantum efficiency by dye doping, which has led to OLED's that span the entire visible spectrum with reasonably good efficiencies and chromaticities. Even at very low-doping levels, the emission from the doped device comes exclusively from the dye dopant, as a result of efficient energy transfer and/or carrier trapping at the dye dopant. By shifting the emission from the HTL or ETL to the dye, the efficiency of the device can be improved significantly. This quantum efficiency increase is due largely to the improved luminescence efficiency of the dispersed dye relative to the dense ETL or HTL that it is doped into. Dye doping often gives significantly narrower EL spectra than nondoped devices. This is a significant benefit in full-color display applications, which require saturated red, green, and blue outputs for color mixing. Dye doping can also lead to significant enhancements in the stability of the OLED as well, preventing crystallization of the glassy HTL or ETL materials. The progress made in developing and identifying new dyes, as well as understanding the mechanism of electroluminescence in these doped devices is very good. There are still many challenges, however, in the design of optimal host and dye materials for the highest efficiencies, most saturated colors and most robust devices [42], [43]–[45].

REFERENCES

[1] M. Pope, H. P. Kallmann, and P. J. Magnante, "Electroluminescence in organic crystals," *J. Chem. Phys.*, vol. 38, p. 2042, 1963.
[2] W. Helfrich and W. G. Schneidere, "Recombination radiation in anthracene crystals," *Phys. Rev. Lett.*, vol. 14, p. 229, 1965.
[3] P. Mark and W. Helfrich, "Space-charge-limited currents in organic crystals," *J. Appl. Phys.*, vol. 33, p. 205, 1962.
[4] J. Dresner, "Double injection electroluminescence in anthracene," *RCA Rev.*, vol. 30, p. 322, 1969.
[5] C. W. Tang and S. A. VanSlyke, "Organic electroluminescent diodes," *Appl. Phys. Lett.*, vol. 51, p. 913, 1987.
[6] ———, "Electroluminescence of doped organic thin films," *J. Appl. Phys.*, vol. 65, p. 3610, 1989.
[7] S. P. Sibley, M. E. Thompson, P. E. Burrows, and S. R. Forrest, "Electroluminescence in molecular materials," in *Optoelectronic Properties of Inorganic Compounds*, D. M. Roundhill, and J. Fackler, Eds. New York: Plenum, in press.
[8] L. J. Rothberg and A. J. Lovinger, "Status of and prospects for organic electroluminescence," *J. Mater. Res.*, vol. 11, p. 3174, 1996.
[9] C. W. Tang, "Organic electroluminescent materials and devices," in *Dig. 1996 SID Int. Symp.,*, SID, San Diego, CA, 1996, p. 181.
[10] ———, "Organic electroluminescent materials and devices," *Inform. Display*, vol. 10, p. 16, 1996.
[11] A. Shoustikov, Y. You, P. E. Burrows, M. E. Thompson, and S. R. Forrest, "Orange and red organic light-emitting devices using aluminum tris(5-hydroxyquinoxaline)," *Synth. Metals*, vol.91, pp. 217–221, 1997.
[12] H. Suzuki, and S. J. Hoshino, "Effects of doping dyes on the electroluminescent characteristics of multilayer organic light-emitting diodes," *Appl. Phys.*, vol. 79, p. 8816, 1996.
[13] D. J. Fatemi, H. Murata, C. D. Merritt, and Z. H. Kafafi, "Highly fluorescent molecular organic composites for light-emitting diodes," *Synth. Metals*, vol. 85, p. 1225, 1997.
[14] Y. Sato, S. Ichinosawa, and H. Kanai, *Inorganic and Organic Electroluminescence/EL*, H. E. Gumlich and R. H. Mauch, Eds., Berlin, Germany, 1996, p. 385.
[15] J. Kido, and J. Endo, "A novel electroluminescent metal complex: Tris(4-phenanthridinolato)aluminum(iii)," *Chem. Lett.* 1997, vol. 7, p. 593, 1997; see also "Orange color electroluminescence from bis(2-styryl-8-quinolinolato)zinc(ii)," *Chem. Lett.* 1997, vol. 7, p. 633, 1997.
[16] C. Wu, J. C. Sturm, R. A. Register, J. Tian, E. P. Dana, and M. E. Thompson, "Efficient organic electroluminescent devices using single-layer doped polymer thin films with bipolar carrier transport abilities," *IEEE Trans. Electron Devices*, vol. 44, p. 1269, 1997.
[17] S. A. Van Slyke, C. H. Chen, and C. W. Tang, "Organic electroluminescent devices with improved stability," *Appl. Phys. Lett.* vol. 69, p. 2160, 1996.
[18] J. Kido, H. Hayase, K. Hongawa, K. Nagai, and K. Okuyama, "Bright red light-emitting organic electroluminescent devices having a europium complex as an emitter," *Appl. Phys. Lett.*, vol. 65, p. 2124, 1994.
[19] M. Pope and C. E. Swenberg, *Electronic Processes in Organic Crystals*. Oxford, U.K.: Clarendon, 1982.
[20] D. Z. Garbuzov, S. R. Forrest, A. G. Tsekoun, P. E. Burrows, V. Bulovic, and M. E. Thompson, "Organic films deposited on Si p-n junctions: accurate measurements of fluorescence internal efficiency, and application to luminescent antireflection coatings," *J. Appl. Phys.*, vol. 80, p. 4644, 1996.
[21] C. Adachi, T. Tsutsui, and S. Saito, "Blue light-emitting organic electroluminescent devices," *Appl. Phys. Lett.*, vol. 56, p. 799, 1990.
[22] Y. Hamada, T. Sano, K. Shibata, and K. Kuroki, "Influence of the emission site on the running durability of organic electroluminescent devices," *Jpn. J. Appl. Phys.*, vol. 34, pt. 2, p. L824, 1995.
[23] Y. Hamada, "The development of chelate metal complexes as an organic electroluminescent material," *IEEE Trans. Electron Devices*, vol. 44, p. 1208, 1997.
[24] E. Aminaka, T. Tsutsui, and S. Saito, "Effect of layered structures on the location of emissive regions in organic electroluminescent devices," *J. Appl. Phys.*, vol. 79, p. 8808, 1996.
[25] A. Gilbert and J. Baggott, *Essentials of Molecular Photochemistry*, 1st ed. Oxford, U.K.: Blackwell Scientific, 1991, p. 173.
[26] J. B. Birks, *Photophysics of Aromatic Molecules*. London, U.K.: Wiley-Interscience, 1970, p. 569.
[27] R. G. Bennett, "Radiationless intermolecular energy transfer. I. Singlet-singlet transfer," *J. Chem. Phys.*, vol. 41, pp. 3037-3041, 1964.
[28] S. Saito, T. Tsutsui, M. Era, N. Takada, C. Adachi, Y. Hamada, and T. Wakimoto, "Progress in organic multilayer electroluminescent devices," in *Proc. SPIE*, 1993, vol. 1910, p. 212.
[29] D. L. Dexter, "A theory of sensitized luminescence in solids," *J. Chem. Phys.*, vol. 21, pp. 836–850, 1953.
[30] N. J. Turro, *Modern Molecular Photochemistry*. Menlo Park, CA: Benjamin/Cummings, 1978.

[31] A. Edwards, C. Claude, I. Sokolik, T. Y. Chu, Y. Okamoto, and R. Dorsinville, "Photoluminescence and electroluminescence of new lanthanide-(methoxybenzoyl)benzoate complexes," *J. Appl. Phys.*, vol. 82, p. 1841, 1997.

[32] T. Sano, M. Fujita, T. Fujii, and Y. Hamada, "Novel europium complex for electroluminescent devices with sharp red emission," *Jpn. J. Appl. Phys.*, pt. 1, no. 4A, p. 1883, 1995.

[33] J. Kido, H. Hayase, K. Hongawa, and K. Nagai, "Bright red light-emitting organic electroluminescent devices having a europium complex as an emitter," *Appl. Phys. Lett.*, vol. 65, p. 2124, 1994.

[34] J. Kido, K. Nagai, Y. Okamoto, and T. Skotheim, "Electroluminescence from polysilane film doped with europium complex," *Chem. Lett.*, 1991, p. 1267.

[35] W. Dawson, J. Kropp, and M. Windsor, "Internal-energy-transfer efficiencies in Eu3+ and Tb3+ chelates using excitation to selected ion levels," *J. Chem. Phys.*, vol. 45, p. 2410, 1966.

[36] H. J. A. Dartnall, J. K. Bowmaker, and J. D. Mollon, "Human visual pigments: Microspectrophotometric results from the eyes of seven persons," *Proc. Roy. Soc. Lon. B*, vol. 220, pp. 115–130, 1983.

[37] B. D. Gupta, and I. C. Goyal, "Absorption of light by visual pigments: A review of theoretical analyses," *J. Photochem.*, vol. 30, p. 173, 1985.

[38] H. Zollinger, *Color Chemistry*, 2nd ed. Weinheim, Germany: VCH Verlagsgesellschaft mbH, 1991, p. 41.

[39] A. N. Netravali, and B. G. Haskell, *Digital Pictures, Representation and Compression*. New York: Plenum, 1988.

[40] J. Kido, K. Hongawa, K. Okuyama, and K. Nagai, "White light-emitting organic electroluminescent devices using the poly(N-vinylcarbazole) emitter layer doped with three fluorescent dyes," *Appl. Phys. Lett.*, vol. 64, p. 815, 1994.

[41] J. Kido, M. Kimura, and K. Nagai, "Multilayer white light-emitting organic electroluminescent device," *Science*, vol. 267, p. 1332, 1995.

[42] C. Hosokawa, H. Higashi, H. Nakamura, and T. Kusumoto, "Highly efficient blue electroluminescence from a distyrylarylene emitting layer with a new dopant," *Appl. Phys. Lett.*, vol. 67, p. 3853, 1995.

[43] M. Takeuchi, H. Masui, I. Kikuma, M. Masui, T. Muranoi, and T. Wada, "Effects of anthracene doping on electrical and light-emitting behavior of 8-hydroxyquinoline-aluminum-based electroluminescent devices," *Jpn. J. Appl. Phys.*, vol. 31, p. L498, 1992.

[44] H. Suzuki, H. Meyer, S. Hoshino, and D. Haarer, "Electroluminescence from multilayer organic light-emitting diodes using poly(methylphenylsilane) as hole transporting material," *J. Appl. Phys.*, vol. 78, p. 2684, 1995.

[45] P. E. Burrows, S. R. Forrest, M. E. Thompson, and S. P. Sibley, "Color-tunable organic light-emitting devices," *Appl. Phys. Lett.*, vol. 69, p. 2959, 1996.

[46] M. E. Thompson and Y. You, unpublished results.

Andrei A. Shoustikov received the M.S. degree in chemical engineering from Moscow D. Mendeleyev University of Chemical Technology, Russia, in 1993, and is working towards the Ph.D. degree in chemistry from the University of Southern California, Los Angeles.

Since 1996, he has been carrying out research at USC in fabrication and characterization of organic light-emitting devices in a group led by Prof. M. Thompson.

Yujian You received the B.S. degree in chemistry from Nanjing University, Nanjing, China, and the Ph.D. degree in chemistry from the University of Illinois, Urbana-Champaign, in 1996.

Since 1996, he is a Post-Doctoral Fellow in the Department of Chemistry, University of Southern California, Los Angeles, CA, where he is carrying out research in fabrication and characterization of organic light-emitting devices.

Mark E. Thompson graduated from the University of California at Berkeley in 1980, and received the Ph.D. degree in chemistry from the California Institute of Technology, Pasadena, CA, in 1985.

He then took an S.E.R.C. Post-Doctoral Fellowship with Prof. M. Green in the Inorganic Chemistry Laboratory at the University of Oxford, U.K., working on projects involving layered organometallic materials and the study of new materials for nonlinear optics. In 1987, he joined the faculty of the Chemistry Department at Princeton University, Princeton, NJ, as an Assistant Professor. In June 1995, he took an Associate Professor's position at the University of Southern California. His research is aimed at understanding the optical, electronic, and catalytic properties of novel organic and metal–organic materials.